Life Sciences in Space Research xxx (xxxx) xxx

Contents lists available at ScienceDirect

Life Sciences in Space Research

journal homepage: www.elsevier.com/locate/lssr

Feasibility of portable Raman SERS for blood biomarker monitoring in spaceflight conditions

Hayley N. Brawley [a,1,*], Isaac D. Juárez [b], Dmitry Kurouski [b], Sara R. Zwart [c], Scott M. Smith [d]

[a] JES Tech, Houston, TX, USA
[b] Department of Biochemistry & Biophysics, Texas A&M University, College Station, TX, USA
[c] University of Texas Medical Branch, Galveston, TX, USA
[d] Human Health and Performance Directorate, NASA Johnson Space Center, Houston, TX, USA

ARTICLE INFO

Keywords:
Biomarkers
Spaceflight
Nanoparticles
Portable
Raman spectroscopy

ABSTRACT

Raman spectroscopy has gained prominence in biological and medical applications due to its ability to detect biomolecules in a non-destructive and real-time manner. This is particularly valuable for space missions, where in situ biomarker analysis is crucial for monitoring astronaut health on missions where timely sample return is not possible. The challenges associated with detecting low-abundance biomarkers in a complex biological matrix, such as blood, can be addressed through surface-enhanced Raman scattering (SERS) using gold nanoparticles (AuNPs). This study represents a ground-based preliminary investigation into the use of SERS in combination with portable Raman spectroscopy for in situ blood biomarker detection. We aimed to assess whether signal enhancement could be achieved using the Agilent Vaya™ Raman spectrometer with AuNPs, under minimal sample processing conditions. The handheld portable device reliably captured albumin-dominated Raman spectra from both serum and plasma. When combined with AuNPs, SERS amplification revealed additional weak spectral bands, presumably from low-abundance biomolecules otherwise masked by dominant protein signals, resulting in an average signal increase of 67 %. These findings demonstrate that portable SERS-based Raman spectroscopy can uncover subtle biochemical information from complex, unfiltered samples, supporting its utility for future real-time biomarker monitoring in resource-limited environments such as spaceflight.

1. Introduction

In situ health monitoring is a critical need for future exploration-class space missions. Astronauts on these missions will be increasingly isolated from terrestrial medical infrastructure and subjected to unique stressors, including ionizing radiation, altered gravity, and confinement (Patel et al., 2020). The ability to perform onboard biological assessments would support detection of health issues and inform medical decisions without the need to return samples to Earth. Currently, blood samples collected on the International Space Station (ISS) are frozen and returned for post-mission analysis, highlighting a significant gap in the capacity for real-time physiological monitoring.

Among candidate technologies, Raman spectroscopy is attractive due to its ability to provide non-destructive, label-free chemical analysis with minimal sample preparation. Raman spectroscopy detects inelastic scattering of monochromatic light, which generates a molecular fingerprint based on vibrational energy transitions (Smith et al., 2004). In biological systems, it has been used to characterize cells, tissues, and biofluids, including blood (Volkov et al., 2022; Atkins et al., 2017). However, conventional Raman spectroscopy suffers from low sensitivity due to the inherently weak scattering process. This limitation can be overcome by surface-enhanced Raman scattering (SERS), a technique that uses metal nanoparticles, commonly gold (AuNPs) or silver, to amplify Raman signals by orders of magnitude (Sharma et al., 2012). Numerous studies have already demonstrated the utility of both Raman and SERS for blood biomarker detection (Milan et al., 2022; Aldosari, 2022). For instance, prior work has used these techniques to identify molecular changes in blood associated with cancer (Neugebauer et al.,

Abbreviations: SERS, Surface-enhanced Raman spectroscopy; SORS, Spatially offset Raman spectroscopy; NP, Nanoparticle; AuNP, Gold nanoparticle.

* Corresponding author.
E-mail address: hayley.n.brawley.ctr@health.mil (H.N. Brawley).
[1] Present address: Clinical and Operational Space Medicine Innovation Consortium, 59th Medical Wing Science & Technology, Lackland Air Force Base, Texas.

https://doi.org/10.1016/j.lssr.2025.11.013
Received 8 July 2025; Received in revised form 23 November 2025; Accepted 26 November 2025
Available online 27 November 2025

2010), anemia (da Silva et al., 2019), diabetes (Birech et al., 2017), and other physiological states. Thus, neither SERS nor portable Raman instrumentation is novel in the context of blood analysis.

Nonetheless, spaceflight-relevant adaptations of these techniques remain limited. Most prior work has relied on benchtop Raman systems and controlled laboratory conditions, often requiring filtered samples, extended incubation, or complex substrates. Furthermore, no current Raman or SERS instrumentation is deployed on the ISS for biomedical use. Given this gap, there is growing interest in evaluating whether portable Raman devices – especially those with integrated SERS capability – can be adapted for low-volume, real-time analysis in austere environments such as spacecraft.

Portable Raman systems face several practical challenges: limited spectral resolution and power compared to benchtop systems, inconsistent sample-laser alignment, and poor reproducibility of signal enhancement in complex matrices like blood (Wang et al., 2022). Horizontal sampling geometries typical of handheld systems can introduce additional variability, especially when analyzing liquids, as surface fluctuations affect focal alignment (Sun et al., 2020). Moreover, protein-rich fluids like plasma and serum often mask low-abundance signals and suppress enhancement effects unless samples are pretreated or filtered (Bonifacio et al., 2014).

This study was designed as a preliminary investigation into these challenges. We evaluated a commercially available handheld Raman spectrometer (Agilent Vaya™) that employs spatially offset Raman spectroscopy (SORS), a modality that improves signal acquisition by probing deeper into the sample and minimizing surface interference (Esparza et al., 2019). Our objective was twofold: (Patel et al., 2020) to assess whether SERS signal enhancement could be achieved in unprocessed human serum and plasma using gold nanoparticles under simplified, spaceflight-relevant conditions including no filtration, minimal sample volume, limited mixing, and no extended incubation, and (Smith et al., 2004) to evaluate whether a portable Raman system could reliably capture biomolecular signatures in blood components using a simplified workflow. While this study was conducted terrestrially, it parallels the operational constraints encountered during spaceflight and serves as an early-stage evaluation of the potential for in situ blood analysis aboard spacecraft. By characterizing spectra with and without SERS, we aimed to determine whether this combined approach could provide meaningful, real-time physiological readouts suitable for future space medicine applications.

2. Materials and methods

2.1. Subjects and blood collection

This protocol was reviewed and approved by the NASA Institutional Review Board and all subjects provided written informed consent prior to participation. Eight healthy, non-smoking adult participants (3 females, 5 males) provided a non-fasting blood sample twice, approximately two weeks apart. During phlebotomy, blood samples (8 mL at each session) were collected into appropriate tubes (1x 3 mL K2-EDTA (BD Vacutainer) and 1x 5 mL serum separator (BD Vacutainer)) and processed to yield whole blood, plasma, or serum. Specimens were aliquoted into sterile cryovials (Fisher Scientific) and frozen at −80 °C until tested.

2.2. Nanoparticle synthesis

Gold (III) chloride trihydrate ($HAuCl_4 \times 3H_2O$), trisodium citrate ($Na_3C_6H_5O_7 \times 2H_2O$), and phosphate buffered saline (PBS) were purchased from Sigma-Aldrich (St. Louis, MO). A 0.5 % gold (III) chloride solution was prepared with deionized water (DiH_2O), and a 1 % trisodium citrate was prepared fresh with DiH_2O. AuNPs were synthesized similarly to a previously published method (Esparza et al., 2019). Briefly, 100 μL of 0.5 % gold (III) chloride solution to 4.9 mL of DiH_2O; this solution was brought to a boil while stirring on a magnetic hot plate. Once boiling, ~40 μL of 1 % trisodium citrate solution was added to the mixture while still stirring. The reaction was allowed to go to completion (i.e., no further color change), and boiling continued for an additional 10 min. The colloidal gold was cooled to room temperature (RT) and then centrifuged at 3000x*g* for 30 min. The pellet was resuspended in 5 mL of 10 mM PBS pH 7.4 (Esparza et al., 2019). Absorbance of the AuNPs was confirmed by UV–Visible spectroscopy (SpectraMax Plus 384, Molecular Devices, San Jose, CA). Peak absorbance near 540 nm (Figure S1) indicates presence of monomeric nanoparticles with an approximate size of 55 nm.

2.3. Sample preparation

To validate the handheld Raman spectrometer's ability to accurately measure the Raman spectra of biomolecules, citric acid was chosen due to its key role in the Krebs cycle (Nelson et al., 2017), its high concentration in cells and blood (Iacobazzi et al., 2014; Parkinson et al., 2021), and its well-documented Raman signature (Huang et al., 2013). Citric acid monohydrate (Sigma-Aldrich, St. Louis, MO) was used to prepare several concentrations of citrate solutions diluted with 18 mΩ▪cm ultrapure water (Milli-Q, Millipore, Billerica, MA). A 100 mg/mL solution of bovine serum albumin (BSA, Sigma-Aldrich, St. Louis, MO) was prepared in ultrapure H_2O.

Citrate standard-nanoparticle solutions were prepared in glass vials (Agilent Technologies, Santa Clara, CA) by diluting the citrate standard to the desired final concentration with 4x volume of nanoparticle solution to a total volume of 1 mL. Solutions were rapidly vortexed to prevent nanoparticle aggregation and a Raman spectrum obtained shortly thereafter.

Sample-nanoparticle solutions were prepared in glass vials (Agilent Technologies, Santa Clara, CA) by diluting serum or plasma samples with 2x volume of nanoparticle solution to a total volume of 1 mL. Control blood solutions were prepared by diluting serum or plasma samples with 2x volume of ultrapure H_2O to a final volume of 1 mL.

For this study, minimal sample processing refers to the absence of pre-filtration, centrifugation beyond routine serum/plasma separation, or incubation steps commonly used in SERS workflows to enhance nanoparticle-analyte interaction. Samples were mixed by vortexing for ~10 s and analyzed immediately.

2.4. Raman instrumentation

All measurements were performed using the Agilent Vaya™ handheld Raman spectrometer (Agilent Technologies, Santa Clara, CA) equipped with an 830 nm excitation laser (450 mW power with an approximate 2.5–3.0 mm beam spot size). A vendor-specific vial adapter and glass vials (4 mL capacity) were utilized to perform all measurements and provided a contained laser setup. Based on limited blood sample and AuNPs volume, we tested the lowest volume required to achieve a detectable, high-fidelity signal with the glass vial and adapter setup (i.e., where the vertical positioning of the incident laser would still reach the sample to produce reproducible scattering. Differing volumes (0.5, 1, 2, and 4 mL) of 50 mM citrate were measured.

Spectra were collected using the glass vial adapter in offset mode (0.6 mm offset) with fixed exposure and scan times. By default, the glass vial adapter collects offset spectra only; zero (conventional Raman) spectra are not acquired unless separately programmed. Both a zero spectrum and an offset spectrum are necessary to leverage the SORS modality. This offset-only method was employed for all subsequent scans, so the SORS functionality was not used in this experiment. The device's spectral range was 350–2000 cm^{-1}, with each scan lasting approximately 50 s. A system check was performed before and after each batch of scans to ensure instrument performance.

2.5. Spectral processing

All spectral processing was performed in MATLAB R2024b (Mathworks, Natick, MA) by importing csv files from the handheld Raman spectrometer. When replicate offset spectra were collected for a sample, spectra were averaged to prepare one representative spectra. All spectra are presented as wavenumber (cm^{-1}) vs. intensity in arbitrary units (a.u.).

A baseline adjustment was performed on applicable datasets such that the minimum value was subtracted from all data points of the individual, raw offset spectra, thereby providing a baseline of zero for comparison. These baseline-adjusted spectra are referred to as "offset spectra" within the text.

To assess for enhancement effects due to SERS, we used a two-step process that involved linear regression and then subsequent baseline adjustment. Initially, we selected a specific range of the data where the baseline was assumed to be approximately linear (typically 750–1000 cm^{-1}). Within this selected range, a linear regression model was fit to estimate the baseline using MATLAB's "polyfit" function. The estimated linear baseline was then subtracted from the entire dataset to remove baseline drift. Then, to normalize the data, we calculated the minimum value of the baseline-corrected dataset and subtracted this value from all data points. This final step ensured that the minimum value of the corrected data was set to zero. The resulting baseline-corrected data is referred to herein as "offset, baseline corrected" spectra.

Integrated spectral counts were calculated using numerical integration with the "trapz" function in MATLAB. Offset, baseline-corrected spectra were integrated over specific Raman shift ranges (as detailed in figure captions), and comparisons were visualized in GraphPad Prism 10.3.1 (GraphPad Software, Boston, MA). Signal enhancement due to the presence of nanoparticles was expressed as percent differences in integrated counts since the precise number of molecules contributing to each signal could not be determined and all acquisition parameters held constant between measurements.

3. Results

3.1. Validating the handheld Raman spectrometer

Raman spectra were collected for an empty 4 mL glass vial, 3.6 g crystalline citric acid, and 4 mL of a 500 mM aqueous citrate standard (Fig. 1). The spectra of crystalline citric acid displayed sharp, intense peaks, notably different from the glass background. In contrast, the aqueous citrate solution exhibited broader spectra due to strong hydrogen bonding in water, which disperses vibrational frequencies (Ojha et al., 2018). The prominent citrate peaks, in both solid and aqueous forms, were those observed at 800 cm^{-1} (795 cm^{-1} in solid) and 942 cm^{-1}. The mode near 800 cm^{-1} is typically attributed to the C—C stretching vibration, and the mode around 942 cm^{-1} is associated with the C—O stretching vibration, particularly involving the carboxylate groups ($-COO^-$) in the citrate ion (Tarakeshwar et al., 1994).

Raman signal generally correlates with concentration (Huang et al., 2013), and thus to assess fidelity of the handheld Raman spectrometer, we determined the linearity of citrate standards. Intensity of the Raman signals associated with citrate increased with the number of molecules in solution (Fig. 2A). Correlation of the two identified Raman peaks' signals and concentration was > 0.98 between 3.125 and 100 mM (Fig. 2B). This linear relationship can be affected by factors such as signal saturation, fluorescence, and molecule aggregation (Smith et al., 2004).

Volumes of $\geq$1 mL produced consistent spectra with <6 % coefficient of variation (CV) after offset and baseline correction in the 760–1000 cm^{-1} range (Figure S2). The 0.5 mL sample's spectrum resembled that of the glass vial alone (Figure S2 vs. Fig. 1). Consequently, a minimum working volume of 1 mL was selected for further AuNP experiments. Additionally, replicate spectra of citrate standards demonstrated a %CV of <1 %.

3.2. Detecting SERS enhancement with the handheld Raman spectrometer

AuNPs were vortexed with 50 mM citrate at a 4:1 ratio with AuNPs in excess, and the Raman spectra captured quickly thereafter. This mixture ratio was selected to maximize interaction sites, attempt uniform coverage, and prevent aggregation. While SERS enhancement is not uniform across the entire Raman spectrum due to the nature of the electromagnetic and chemical enhancement mechanisms involved, enhancement due to SERS was observed for both dominant citrate peaks (Fig. 3A). Although citrate was used as the reducing agent in the AuNP synthesis, we observed negligible Raman signal in AuNPs alone (Fig. 3A), indicating minimal interference from residual surface-bound citrate in the absence of free citrate in solution. Therefore, signal enhancement observed in citrate-AuNP mixtures is attributable to added citrate standards, not residual citrate from nanoparticle preparation. Enhancement was subsequently quantified for each peak (Fig. 3B), with a resulting increase in signal of 26–30 %. When this experiment was repeated with 16.7 and 20 mM citrate, enhancement was again

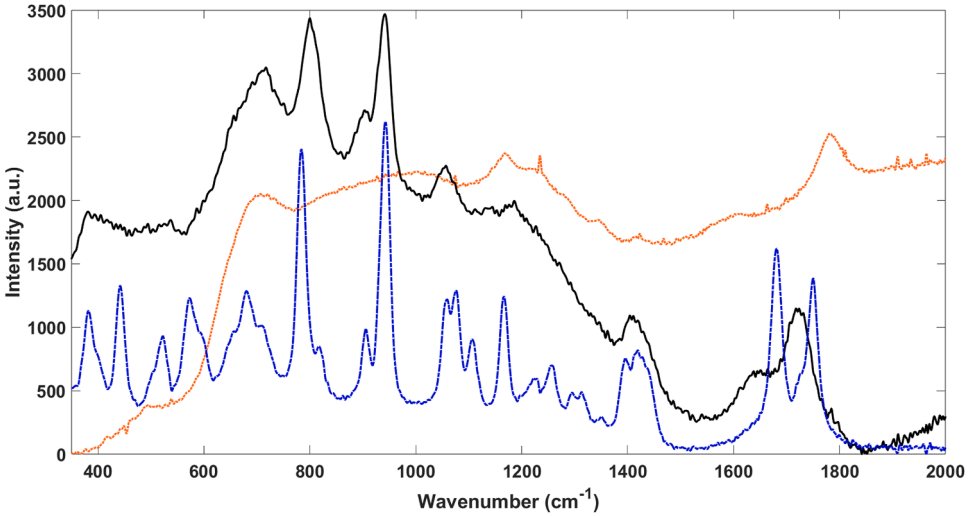

Fig. 1. Raman signal from citrate and vial materials. offset Raman spectra of an empty glass vial (orange, dotted), 500 mM citrate in a glass vial (black, solid), and 3.6 g citric acid monohydrate crystalline solid in a glass vial (blue, dashed). Spectra of the crystalline solid citric acid has been reduced by a factor of 10.

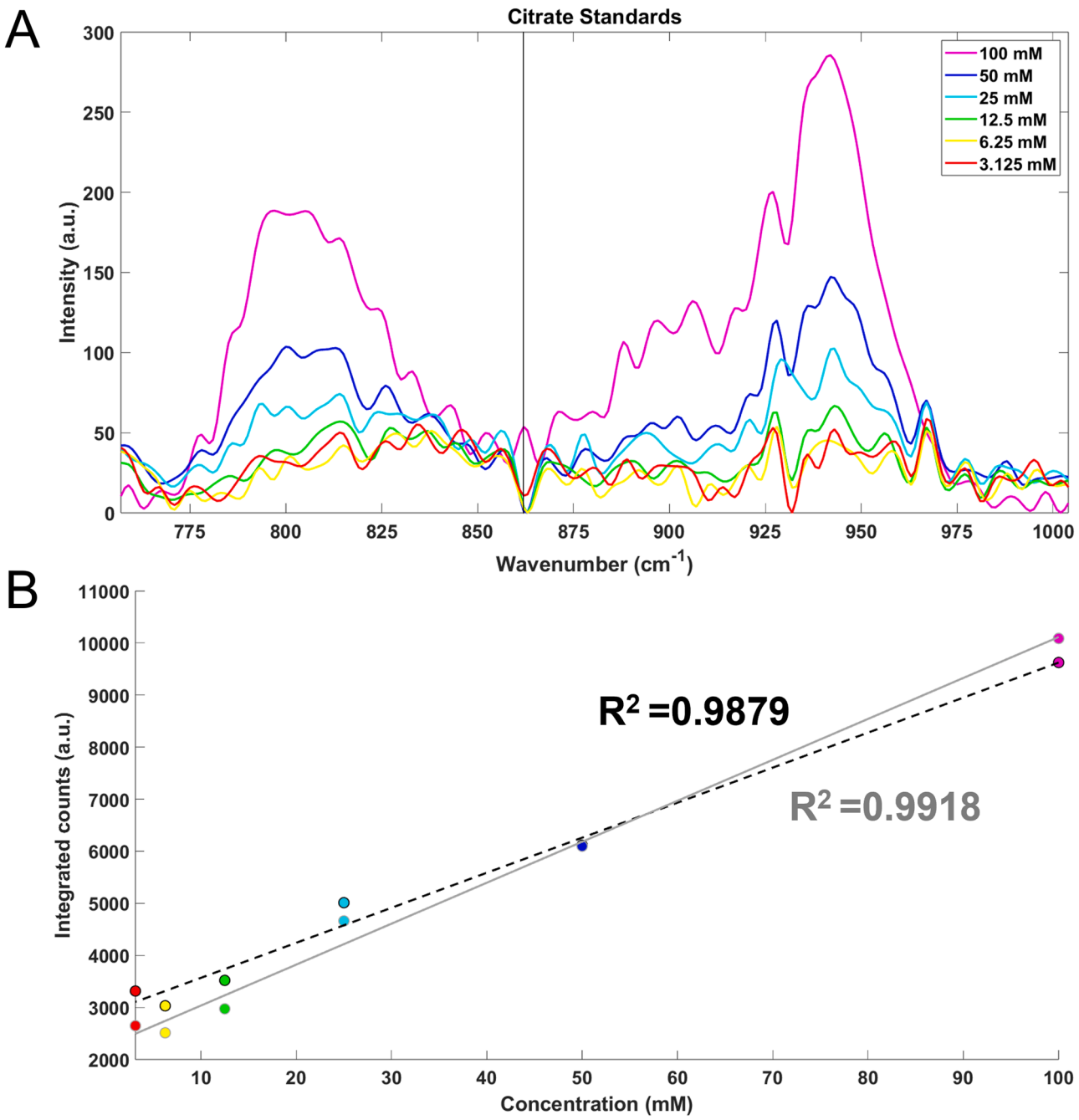

Fig. 2. Linearity of citrate detection by Raman. (A) Offset, baseline corrected Raman spectra of citrate standards (3.125–100 mM) in 760–1000 cm^{-1} range and (B) linear regression of integrated counts for the 800 cm^{-1} (black, dashed) and 942 cm^{-1} peaks of citrate (grey, solid).

achieved, albeit to different levels (Table S1). Across all three experiments, the C—C stretching mode at 800 cm^{-1} demonstrated greater enhancement than did the C—O stretching mode at 942 cm^{-1}, suggesting selective enhancement of specific vibrational modes (Moskovits, 1985).

Additionally, citrate standards were incubated for 1 and 2 hr at room temperature without agitation following initial mixing. After rapidly vortexing prior to re-measurement, the average signal enhancement amongst the two citrate peaks (across two standards) was 22 % and 77 % for 1- and 2-hr incubations, respectively (data not shown). However, there were no discernible trends correlating incubation time with signal enhancement as enhancement of 26–83 % was observed without incubation.

3.3. Blood profiling using the handheld Raman spectrometer

Limited differences in spectral features were observed in serum spectra, whereas spectral features varied, both in observation and intensity, amongst the individual plasma spectra (Fig. 4A and B). Due to blood volume constraints, whole blood was pooled from the eight individuals in order to obtain a large enough volume to sample. The individual sera and plasma spectra were averaged to give representative serum and plasma spectra and are compared to whole blood (Fig. 4C). Isolated hemoglobin has been well characterized using Raman spectroscopy (Hu et al., 1996), and even oxygenated vs. deoxygenated hemoglobin has been distinguished using this technique (Brunner et al., 1972). The Raman signal from the pooled whole blood was weak, but spectral features reminiscent of hemoglobin (at 567, 754, 1582, and

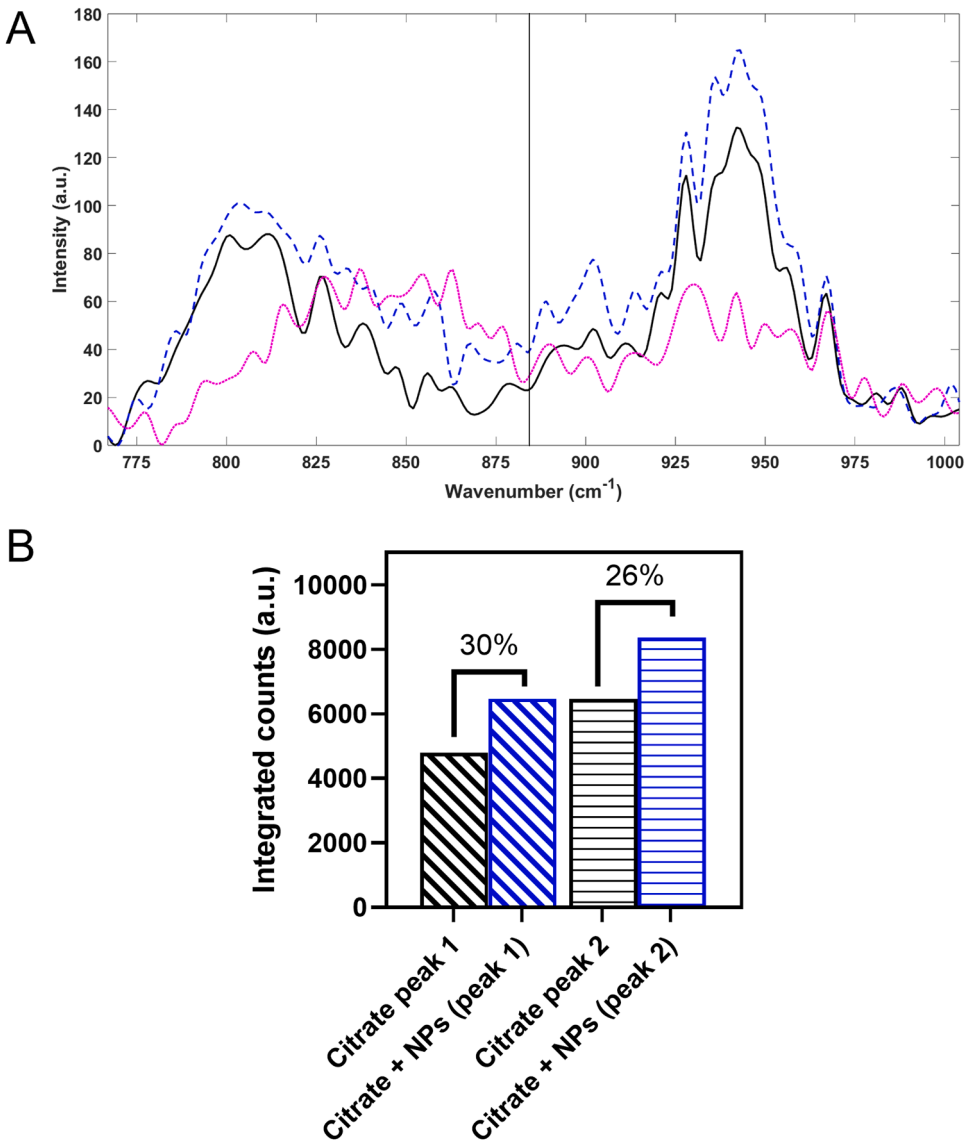

Fig. 3. SERS enhancement of citrate with AuNPs. (A) Offset, baseline corrected Raman spectra of 50 mM citrate with (blue, dashed) or without AuNPs (black, solid) along with spectra of AuNPs alone (magenta, dotted) in 760–1000 cm^{-1} range. (B) Integrated counts under citrate peak #1 (800 cm^{-1}) and peak #2 (942 cm^{-1}) for 50 mM citrate standard with and without AuNPs measured rapidly after mixing. Percent enhancement expressed as percent difference compared to standard is overlaid.

1639 cm^{-1}) were observable.

The averaged blood component spectra were compared to that of bovine serum albumin (BSA) (Fig. 4C). Albumin is a hepatic protein that is important in maintaining vascular oncotic pressure while transporting hormones, vitamins, and other substances throughout the bloodstream. It is the most abundant protein in human blood plasma and has been well characterized via Raman spectroscopy (Artemyev et al., 2016). The BSA Raman spectrum mirrored that of literature with distinct peaks at the amide I band (~1655 cm^{-1}), the CH_2 deformation band (~1447 cm^{-1}), the phenylalanine band (~1002 cm^{-1}), and the tyrosine doublet (~828 and 850 cm^{-1}) (Spedalieri et al., 2023). Both the averaged serum and plasma spectra showed similarity to this standard, suggesting that these spectra are likely dominated by albumin.

3.4. Detecting SERS enhancement within blood components

Lastly, AuNPs were mixed with serum and plasma samples from one individual, and the resulting spectra were compared to those of the same samples diluted with ultrapure H_2O (Fig. 5). After applying offset and baseline correction, the SERS enhancement was quantified in the approximate carotenoid/amino acid (830–1300 cm^{-1}) and amide band (1400–1800 cm^{-1}) regions. For serum, Raman signal intensity increased by 50 % in the carotenoid/amino acid region and 41 % in the amide region relative to the control without AuNPs. For plasma, enhancement was 68 % in the amino acid region and 107 % in the amide region. The strong enhancement observed in the amide region of plasma corresponds to the appearance of previously undetectable low-abundance molecular features, suggesting that AuNPs facilitated selective amplification of protein- and peptide-associated vibrations. Across the four measurements, signal increases ranged from 41 to 107 %, corresponding to an average enhancement of ~67 %.

5. Discussion

This project served as a preliminary investigation into the feasibility of using a handheld Raman spectrometer with and without surface-enhanced Raman spectroscopy (SERS) to detect blood biomolecular signatures, under simplified conditions that mirror constraints encountered in spaceflight. A key goal was to determine whether signal enhancement could be achieved with minimal sample preparation, no

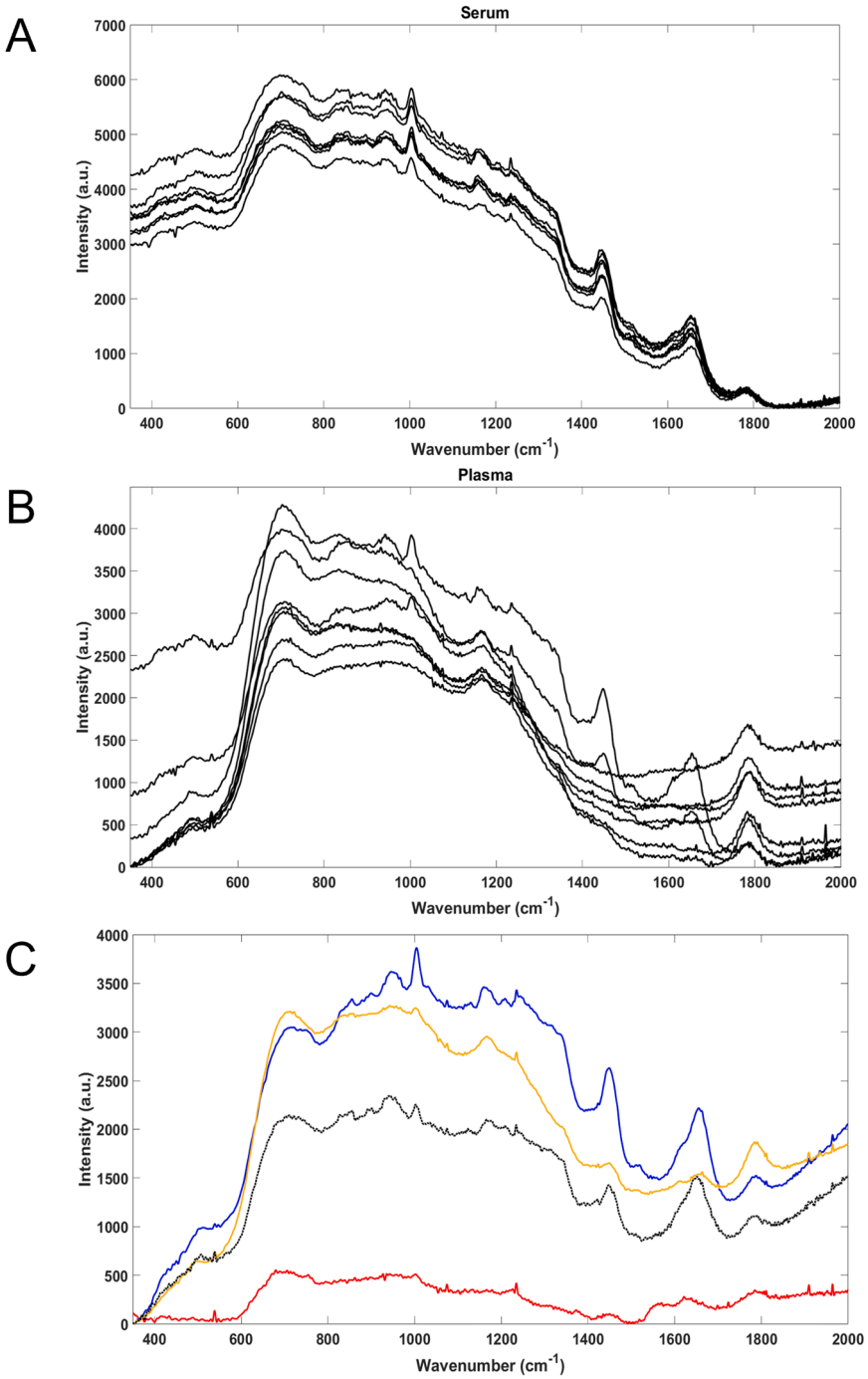

Fig. 4. Blood Component Spectra and Comparison to Albumin. Offset Raman spectra of individual (A) serum (n = 8) and plasma (n = 8) samples, (C) Offset, baseline corrected Raman spectra of averaged serum (from A) (blue, solid), plasma (from B) (orange, solid), whole blood sample that was prepared by pooling equal volumes of each subjects' blood (red, solid) all compared to a 100 mg/mL Bovine Serum Albumin (BSA) standard (black, dotted).

filtration, limited incubation, and using a contained laser setup, specifically the vial and adapter system unique to the Agilent Vaya™ handheld Raman spectrometer. This configuration mitigated horizontal sampling challenges by ensuring consistent sample positioning and laser focus (Sun et al., 2020).

The study began by validating the handheld device's performance with well-characterized standards, including citric acid in solid and aqueous forms. Raman spectra obtained using the device's 830 nm excitation laser were comparable to those obtained using traditional confocal Raman spectroscopy with a 785 nm laser (Huang et al., 2013). Slight spectral differences are attributed to variations in chemical formulation of the standards, differences in instrumentation parameters, and/or distinct substrates affecting optical interference. A linear concentration dependence of the citrate peaks confirmed the instrument's reliability for quantitative measurements. Furthermore, repeatability of spectra collected from the same solution was high, with peak intensity variations typically <1 % CV, consistent with findings in similar handheld Raman systems (Thayer et al., 2019).

We next evaluated whether SERS enhancement could be reliably detected with this device using AuNPs. Gold nanoparticles were selected over silver due to their greater stability, oxidative resistance, ease of surface functionalization, and favorable control over morphology

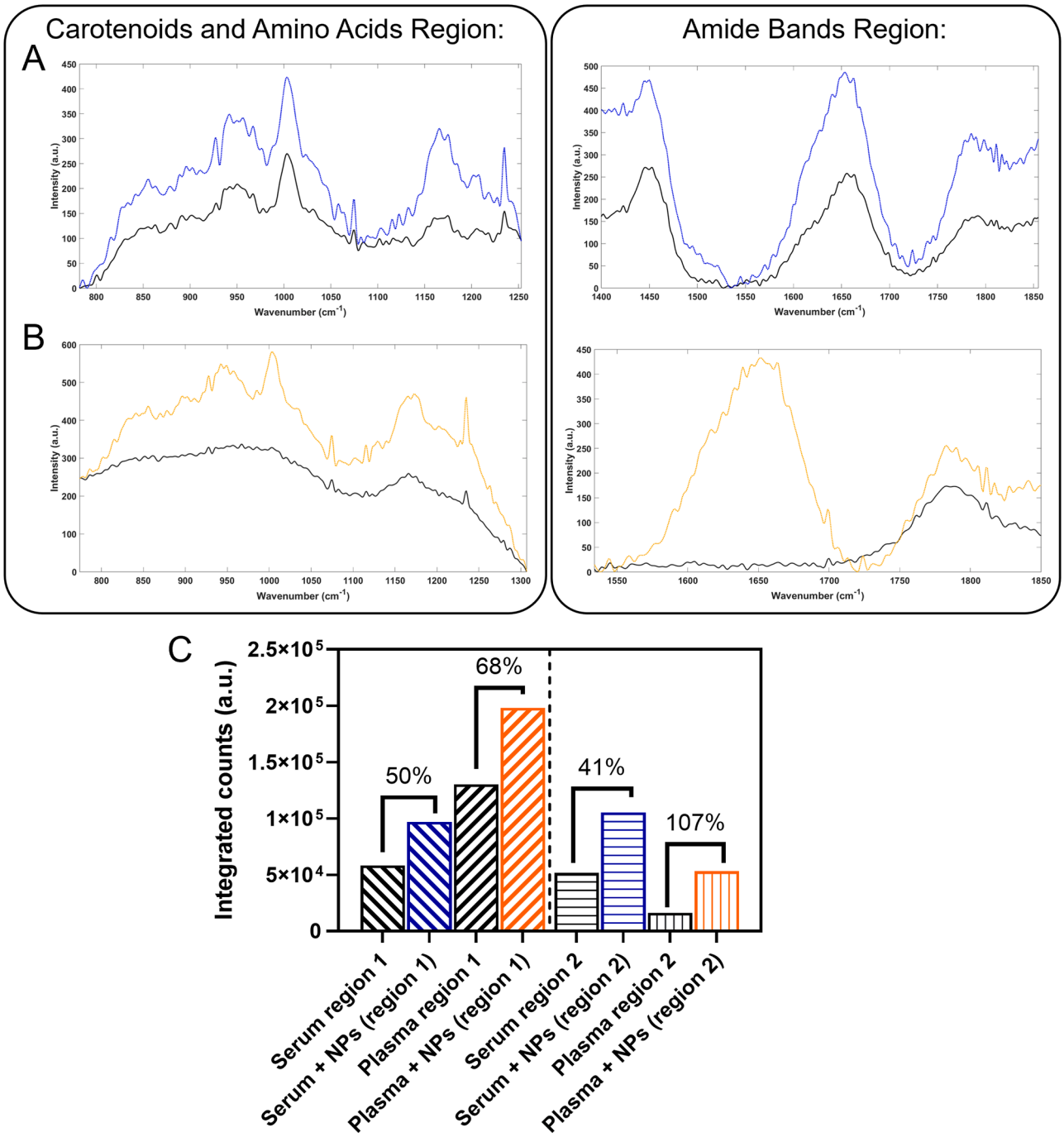

Fig. 5. Nanoparticle-enhanced Detection of Blood Biomolecules. Offset Raman spectra of (A) serum (n = 1) (blue, dotted) and (B) plasma (n = 1) (orange, dotted) from the same subject, with and without AuNPs (black, solid) in both the carotenoids and amino acids region (region 1, 750–1300 cm^{-1}) and the amide bands region (region 2, 1400–1850 cm^{-1}), (C) integrated counts under either region 1 or region 2 for serum and plasma, respectively. Percent enhancement expressed as percent difference is overlaid.

during synthesis (Daniel et al., 2004). When mixed with citrate standards of three different concentrations, the AuNPs consistently enhanced Raman signals, with magnitudes ranging from 26 % to 83 %, depending on concentration. These percent differences, while modest relative to typical SERS enhancement factors (which often range from 10^3 to 10^8 in optimized systems), are consistent with ensemble-averaged measurements in biological fluids where only a small subset of molecules interacts directly with nanoparticle "hot spots". The variability in enhancement is likely attributable to factors such as nanoparticle aggregation, heterogeneity in size and shape, and dynamic interactions with the local chemical environment (e.g., pH, ionic strength, competing solutes) (Wustholz et al., 2010; Kurouski et al., 2016; Pellegrino et al., 2005), all of which influence plasmonic resonance and hotspot formation. Importantly, control experiments confirmed that the AuNPs themselves did not contribute to the background signal, supporting the conclusion that observed signal increases were due to SERS amplification rather than additive spectral contributions.

We tested two nanoparticle-to-analyte mixing ratios (4:1 for citrate, 2:1 for blood samples) based on a review of existing literature (Chen et al., 2019) and the practical constraints of limiting AuNP volume. Enhancement was observed in both scenarios, demonstrating that even rapid vortexing immediately before acquisition, without incubation,

could produce detectable and reproducible enhancement. This finding has significant implications for spaceflight applications, where time and resource constraints demand minimal sample handling. Further studies are required to identify the minimal excess ratio of nanoparticles to sample that maximizes efficiency, ensuring the least possible sample usage, while still achieving optimal enhancement.

When applied to unfiltered serum and plasma samples, the handheld spectrometer captured dominant protein features, primarily from albumin. This success is attributed to the use of the 830 nm near-infrared excitation, which reduces fluorescence from biological matrices and minimizes photodamage. While the degree of enhancement varied between individuals and sample types, we observed consistent amplification of spectral features, particularly within the amide band region (1500–1800 cm^{-1}). These findings are noteworthy in light of Bonifacio's study (Bonifacio et al., 2014), which concluded that negligible enhancement could be observed in unfiltered plasma or serum using Ag or Au colloids, even after extended incubation. In contrast, we observed clear enhancement without filtration or incubation, likely due to the higher AuNP-to-sample ratio, rapid mixing, and the use of an 830 nm excitation laser with an offset collection geometry. Both studies found spectra dominated by proteins, reinforcing that Raman profiles of blood components are highly influenced by their most abundant molecular species.

Unlike classical SERS workflows that emphasize filtration, incubation, or immobilization of analytes on engineered substrates to maximize enhancement, our approach intentionally omits these steps to reflect operational constraints. Traditional methods optimize reproducibility and achieve higher enhancement factors, but they rely on controlled bench conditions and are impractical for rapid, in situ measurements. The observation of measurable enhancement in unfiltered serum and plasma under immediate-mixing conditions therefore demonstrates that meaningful biochemical information can still be recovered without the complex preprocessing typically required for SERS. This distinction reframes our workflow not as a simplified substitute, but as an adaptation of Raman methodology designed for resource-limited biomedical monitoring environments such as spaceflight.

In pooled whole blood, signal intensity was weak and primarily attributable to hemoglobin. This likely resulted from the high laser power (450 mW), which may have induced sample degradation, as hemoglobin is known to be sensitive to thermal denaturation above 2 mW excitation (Lemler et al., 2014). Nevertheless, detectable features consistent with hemoglobin's Raman profile were present. In future studies, using lower-power excitation or cooling stages may preserve the native structure of thermally sensitive proteins.

Importantly, mixing AuNPs with plasma or serum revealed spectral features that were previously undetectable without enhancement. The enhancement was more pronounced in the amide region than the carotenoid/amino acid band, suggesting selective amplification of certain vibrational modes. This is consistent with the known mechanisms of SERS: localized surface plasmon resonance generates highly concentrated electromagnetic fields at the nanoparticle surface, amplifying Raman scattering from nearby molecules (Sharma et al., 2012). Additionally, charge transfer interactions and adsorption to the nanoparticle surface further increase analyte signal (Hermanson, 2013; Nie et al., 1997).

Although SERS and portable Raman devices have been extensively studied for blood analysis in terrestrial settings, no such systems have been used aboard the ISS. Nevertheless, in situ biomarker detection is critical for long-duration missions. Emerging biosensors and lab-on-chip systems (Reinsch et al., 2022; Rabbow et al., 2006) offer promising platforms for onboard health monitoring, but are not currently standard for medical diagnostics in space. Likewise, innovations in plasmonic (Li et al., 2025) and fiber-optic (Liu et al., 2023) biosensors highlight the rapid convergence of miniaturization, plasmonic enhancement, and high-sensitivity molecular recognition. Such technologies exemplify the direction of next-generation onboard biosensing, where fiber-integrated or SERS-enabled optics could permit real-time physiological monitoring in resource-limited environments. Portable, SERS-enabled Raman systems could play a complementary role in this emerging landscape. By demonstrating quantifiable signal enhancement in unfiltered serum or plasma samples with minimal processing, we provide evidence that compact, non-destructive devices may capture biologically meaningful signatures under operational constraints. Future work will need to explore the use of functionalized nanoparticles to target specific biomarkers, such as those associated with oxidative stress, immune response, or nutrient metabolism, while adapting the vial system for smaller volumes or blood-spot analysis (< 1 mL) to enhance practicality for space missions where blood draws are limited.

SORS, or spatially offset Raman spectroscopy, refers to a collection geometry in which the excitation and collection points are laterally displaced to enable deeper subsurface sampling. Although the Agilent Vaya™ device is capable of performing SORS, the adapter used in this study employs a fixed offset configuration and not true SORS. This may have limited the depth of signal collection and contributed to the loss of weaker Raman features. Future work will be required to validate full SORS functionality with this adapter to determine whether deeper signal acquisition improves sensitivity in complex biological fluids. Together with the small sample size and high excitation power required for handheld operation, these constraints represent typical limitations of an initial feasibility study rather than intrinsic shortcomings of the technique.

5. Conclusion

This study serves as a foundational investigation into the feasibility of using portable, SERS-enabled Raman spectroscopy for blood profiling under conditions relevant to spaceflight. By validating a portable, handheld Raman spectrometer for the analysis of human serum and plasma, we demonstrated that quantifiable signal enhancement is achievable using AuNPs, even in unfiltered samples and with minimal mixing or incubation. The ability to detect key spectral features, particularly in the amide region, highlights the potential of this simplified workflow to capture biologically meaningful signatures. These results not only support the use of AuNPs to amplify Raman signals in complex fluids but also show that enhancement can be achieved under conditions suitable for real-time, in situ biomarker monitoring. As current spaceflight operations lack onboard blood analytics, this approach represents a step toward enabling autonomous health diagnostics in space and other resource-limited environments. Future studies should focus on targeting specific biomarkers of physiological relevance and adapting this system for smaller volumes to further enhance its applicability in space medicine.

Financial support

The study was supported by the National Aeronautics and Space Administration Center of Innovation Funding.

Statements and declarations

The views expressed are those of the authors and do not reflect the official views or policy of the National Aeronautics and Space Administration. No federal endorsement of the device manufacturer is intended. All authors declared no conflicts of interest.

Ethical considerations

This protocol was reviewed and approved by the NASA Institutional Review Board (#00019876), and all subjects provided written informed consent.

CRediT authorship contribution statement

Hayley N. Brawley: Writing – review & editing, Writing – original draft, Methodology, Investigation, Funding acquisition, Formal analysis, Data curation, Conceptualization. **Isaac D. Juárez:** Investigation. **Dmitry Kurouski:** Writing – review & editing, Methodology, Investigation. **Sara R. Zwart:** Writing – review & editing, Writing – original draft, Funding acquisition, Formal analysis, Conceptualization. **Scott M. Smith:** Writing – review & editing, Writing – original draft, Funding acquisition, Conceptualization.

Declaration of competing interest

The authors declare that they have no known competing financial interests or personal relationships that could have appeared to influence the work reported in this paper.

Acknowledgements

We thank the volunteers who participated in this study for their time and effort in the success of this project. Additionally, we thank and recognize Mark Mabry of Agilent Technologies for the provided instrumentation training and assistance in method development. We extend our gratitude to the National Aeronautics and Space Administration (NASA) Johnson Space Center's Center of Innovation Funding for financial support. We thank the NASA Nutritional Biochemistry Laboratory team, who were responsible for the overall protocol coordination and implementation, sample collection and processing logistics, biochemical analyses, and data management.

Supplementary materials

Supplementary material associated with this article can be found, in the online version, at doi:10.1016/j.lssr.2025.11.013.

References

Aldosari, F.M.M., 2022. Characterization of labeled gold nanoparticles for surface-enhanced raman scattering. Molecules 27.
Artemyev, D.N., et al., 2016. Measurement of human serum albumin concentration using raman spectroscopy setup. Opt. Quant. Electron. 48.
Atkins, C.G., et al., 2017. Raman spectroscopy of blood and blood components. Appl Spectrosc 71, 767–793.
Birech, Z., et al., 2017. Application of raman spectroscopy in type 2 diabetes screening in blood using leucine and isoleucine amino-acids as biomarkers and in comparative anti-diabetic drugs efficacy studies. PLoS One 12, e0185130.
Bonifacio, A., et al., 2014. Surface-enhanced raman spectroscopy of blood plasma and serum using ag and au nanoparticles: a systematic study. Anal. Bioanal. Chem. 406, 2355–2365.
Brunner, H., et al., 1972. Resonance raman scattering on the haem group of oxy- and deoxyhaemoglobin. J. Mol. Biol. 70, 153–156.
Chen, H.Y., et al., 2019. Simultaneous detection of intracellular nitric oxide and peroxynitrite by a surface-enhanced raman scattering nanosensor with dual reactivity. ACS Sens 4, 3234–3239.
da Silva, W.R., et al. (Eds.), 2019. Diagnosing Iron Deficiency Anemia By Raman Spectroscopy Analysis. Springer Singapore, Singapore.
Daniel, M.C., et al., 2004. Gold nanoparticles: assembly, supramolecular chemistry, quantum-size-related properties, and applications toward biology, catalysis, and nanotechnology. Chem. Rev. 104, 293–346.
Esparza, I., et al., 2019. Surface-enhanced raman analysis of underlaying colorants on redyed hair. Anal. Chem. 91, 7313–7318.
Hermanson, G.T., 2013. Chapter 14 - microparticles and nanoparticles. In: Hermanson, G.T. (Ed.), Bioconjugate Techniques, 3rd edition. Academic Press, Boston, pp. 549–587.
Hu, S., et al., 1996. Assignment of protoheme resonance raman spectrum by heme labeling in myoglobin. J. Am. Chem. Soc. 118, 12638–12646.
Huang, Z., et al., 2013. Quantitative determination of citric acid in seminal plasma by using raman spectroscopy. Appl. Spectrosc. 67, 757–760.
Iacobazzi, V., et al., 2014. Citrate–new functions for an old metabolite. Biol. Chem. 395, 387–399.
Kurouski, D., et al., 2016. Unraveling near-field and far-field relationships for 3d sers substrates–a combined experimental and theoretical analysis. Analyst 141, 1779–1788.
Lemler, P., et al., 2014. Nir raman spectra of whole human blood: effects of laser-induced and in vitro hemoglobin denaturation. Anal Bioanal. Chem. 406, 193–200.
Li, X., et al., 2025. Ultralow-limit of detection optical fiber lspr biosensor based on a ring laser for des-γ-carboxy prothrombin detection. Photonics Res. 13.
Liu, X., et al., 2023. Waveflex biosensor-using novel tri-tapered-in-tapered four-core fiber with multimode fiber coupling for detection of aflatoxin b1. J. Lightwave Technol. 41, 7432–7442.
Milan, J., et al., 2022. Treasure on the earth-gold nanoparticles and their biomedical applications. Materials 15.
Moskovits, M., 1985. Surface-enhanced spectroscopy. Rev. Mod. Phys. 57, 783–826.
Nelson, D.L., et al., 2017. Lehninger Principles of Biochemistry, 7th ed. W. H. Freeman.
Neugebauer, U., et al., 2010. Towards detection and identification of circulating tumour cells using raman spectroscopy. Analyst 135, 3178–3182.
Nie, S., et al., 1997. Probing single molecules and single nanoparticles by surface-enhanced raman scattering. Science 275, 1102–1106.
Ojha, D., et al., 2018. On the hydrogen bond strength and vibrational spectroscopy of liquid water. Sci. Rep. 8.
Parkinson, E.K., et al., 2021. Extracellular citrate and metabolic adaptations of cancer cells. Cancer Metastasis Rev. 40, 1073–1091.
Patel, Z.S., et al., 2020. Red risks for a journey to the red planet: the highest priority human health risks for a mission to mars. NPJ Microgravity 6, 33.
Pellegrino, T., et al., 2005. On the development of colloidal nanoparticles towards multifunctional structures and their possible use for biological applications. Small 1, 48–63.
Rabbow, E., et al., 2006. The sos-lux-toxicity-test on the international space station. Res. Microbiol. 157, 30–36.
Reinsch, N., et al., 2022. The biomonitor iii injectable cardiac monitor: clinical experience with a novel injectable cardiac monitor. J. Clin. Med. 11.
Sharma, Y., et al., 2012a. Advanced glycation end products and diabetic retinopathy. J Ocul Biol Dis Infor 5, 63–69.
Sharma, B., et al., 2012b. Sers: materials, applications, and the future. Materials Today 15, 16–25.
Smith, E., et al., 2004a. Introduction, Basic Theory and principles. Modern raman Spectroscopy – a Practical Approach. John Wiley & Sons, pp. 1–21.
Smith, E., et al., 2004b. Introduction, basic theory and principles. Modern Raman Spectroscopy – a Practical Approach. John Wiley & Sons, pp. 1–21.
Spedalieri, C., et al., 2023. Ultraviolet resonance raman spectra of serum albumins. Appl. Spectrosc. 77, 1044–1052.
Sun, J., et al., 2020. Surface-enhanced raman spectroscopy for on-site analysis: a review of recent developments. Luminescence 35, 808–820.
Tarakeshwar, P., et al., 1994. Ground state vibrations of citric acid and the citrate trianion—An ab initio study. Spectrochimica Acta Part A: Molecular Spectroscopy 50, 2327–2343.
Thayer, E., et al., 2019. Signal detection limit of a portable raman spectrometer for the sers detection of gunshot residue. MRS Commun. 9, 948–955.
Volkov, V.V., et al., 2022. Mapping blood biochemistry by raman spectroscopy at the cellular level. Chemical Science 13, 133–140.
Wang, W., et al., 2022. Applications of surface-enhanced raman spectroscopy based on portable raman spectrometers: a review of recent developments. Luminescence 37, 1822–1835.
Wustholz, K.L., et al., 2010. Structure-activity relationships in gold nanoparticle dimers and trimers for surface-enhanced raman spectroscopy. J. Am. Chem. Soc. 132, 10903–10910.